

Morphology and Epitaxial Growth in a Directed Diffusion Model

K.A. Hawick

Computer Science, Institute for Information and Mathematical Sciences,
Massey University, North Shore 102-904, Auckland, New Zealand

email: k.a.hawick@massey.ac.nz

Tel: +64 9 414 0800 Fax: +64 9 441 8181

September 2010

ABSTRACT

The identification and control of morphological variations in surface growth models are important aspects to understand, with applications including electro-deposition and coatings. We develop a surface growth model based on directed-diffusion and controlled by a single parameter – the Peclet number. We present: a fractal-scaling analysis; structural morphology measurements; and component tree-count and root-count results from extensive simulations. We identify a phase transition in the Peclet number at around 0.75 - 1.0 which appears to be linked to morphological variations. We offer a possible explanation for based on percolation effects and suggest some extensions to the model for studying related surface growth systems. We also present some 3-D renderings of the model internal structures.

KEY WORDS

epitaxial growth; morphology; trees; surface growth; directed diffusion.

1 Introduction

It is important to understand and control the structures that grow on surfaces for applications such as: surface coating [1]; permeable surfaces [2]; fabric surfaces [3]; epitaxial growth [4]; mineral surfaces [5]; chemical vapour deposition [6]; electro-deposition [7–9]; and micro-chip fabrication, that vary on length scales from the macroscopic to atomic scales. In this article we describe development of a diffusion-based model on an arbitrary length scale that can model the different morphological structures that form when an incoming flux of material is incident on a surface.

Diffusion based models have been popular in the literature for some decades now, following the very successful diffusion-limited aggregation (DLA) model of Witten and

Sanders [10] developed in the 1980s. These model have been developed by a number of other researchers [11, 12]. Diffusion processes [13] are well understood and characterised. Meakin developed some diffusion-based models [14, 15] for studying growth on surfaces and lines. Some later work on a vapour phase epitaxial growth model [16–18] was constrained to two-dimensional systems and also to very small system sizes due to computation limitations in the 1990s. More recent work considered sedimentary processes in cluster-cluster aggregation [19, 20] and suggested the use of the Peclet number as a model control parameter [21].

Diffusion models exhibit some very rich spatial structures but also show a surprising degree of reductionist scaling [22] behaviour that can be described using power-laws and other parameterisable relationships [23–25]. They are also known to give rise to fractal structures, characterised by a fractal dimension d_f , that is smaller than the embedding Euclidean dimension [26].

A particularly interesting area of study is that of the morphology of the structures that form in diffusion models [27], some of which include: viscous fingering [28]; nanorods [29]; and other surface modifications [30]. The study of growth kinetics is also an interesting area [31] as is that of colloidal and surface deposition effects from gravity [32].

In this present paper we develop a surface growth model based on directed diffusion and which is capable of being simulated at quite large system sizes. We are able to make detailed 3-D visualisation renderings of the interior of a simulated system as well as detailed quantitative measurements of both its bulk and its microscopic structural properties. Figure 1 shows a set of coloured (shaded) trees grown in a system of base 32×32 using the surface growth model.

We describe the model and its parameterisation in Section 2. Some illustrative model configurations are pre-

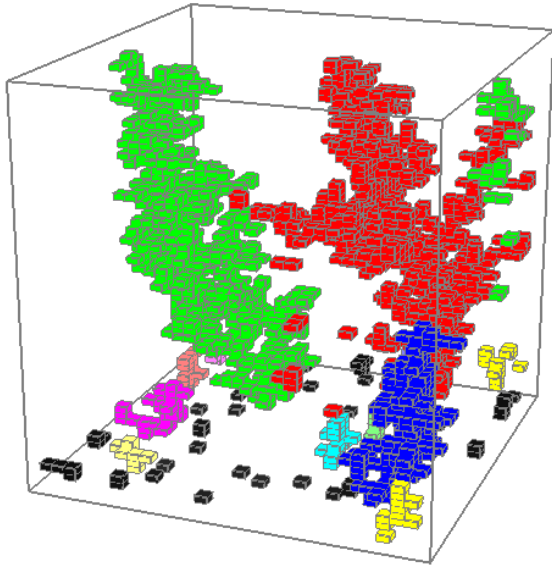


Figure 1: Separated Coloured(shaded) Trees grown from the ground sheet surface with the epitaxial model.

sented in Section 3 as well as plots of measurements such as particle density, component cluster count, fractal dimension and some fitted power laws. Section 4 gives a discussion of the results and some analysis based on a count of the tree cluster size distribution and root-count and some speculations about the influence of percolation effects on tree morphology. A summary and some tentative conclusions are offered in Section 5.

2 Epitaxial Growth Model

We develop a model for epitaxial growth based on a lattice of discrete particle site positions arranged in a box and the filled surface is at the base of the box. Figure 2 shows the schematic of the simulation model, with particles released randomly, and falling through the box until they stick to the surface base, or to another already-stuck walker particle. The epitaxial growth model can be set up using simple diffusion concepts for a single particle, which for simplicity is located on an integer mesh in a recti-linear coordinate space x, y, z with coordinate z giving the height. For convenience the simulated system is “periodic” in the horizontal directions so that particles wrap around if they move too far in x, y . The system is initialised with an empty box apart from a full sheet of filled particles at the base.

Diffusion models can be set up with arbitrary directed diffusion parameters, but it is more useful for subsequent analysis to attempt to characterise the model with as few parameters as possible. We give a brief derivation of a parameter formulation based on mobilities and the Peclet

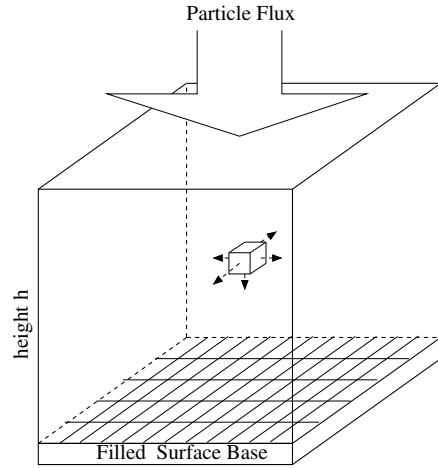


Figure 2: 3-D Box showing particles released randomly from above and falling on a surface box base of filled sites.

number.

Single particle mobility Ω is usually [19] defined as:

$$\Omega = P_{\uparrow} + P_{\downarrow} + P_{\perp} \quad (1)$$

where $P_{\uparrow}, P_{\downarrow}, P_{\perp}$ are diffusion constants proportional to the probabilities of a particle moving up, down, or perpendicular to the gravitational field. It is more useful in the model developed here just to use actual, normalised probabilities where: $p_{\downarrow} = P_{\downarrow}/\Omega, \dots$. A further simplification can be imposed for our present purposes if we disallow the particle to move upwards and set $p_{\uparrow} \equiv 0$. The model has two remaining parameters, and constraining the probability sum to unity, one can be eliminated.

A convenient way to express the remaining model parameter is in terms of the Peclet number P_e , which is given by the relation $P_e = p_{\downarrow}/p_{\perp}$, and is a pure numerical ratio without units. Our model can be expressed in two or three dimensions, and dimension d affects the number of particle movement choices in directions perpendicular to the gravitational field and so given P_e we have:

$$\begin{aligned} p_{\perp} &= \frac{1}{2(d-1) + P_e} \\ p_{\downarrow} &= \frac{P_e}{2(d-1) + P_e} \\ p_{\uparrow} &= 0 \end{aligned} \quad (2)$$

and so for a given particle we can use a single computer-generated uniform random number to determine the direction in which it should move on the recti-linear mesh at a single time step. Figure 3 shows how the model is set up with directionally biased probabilities of movement.

The model algorithm can thus be expressed in summary as:

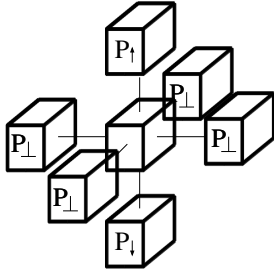


Figure 3: Probabilities of Diffusive Motion

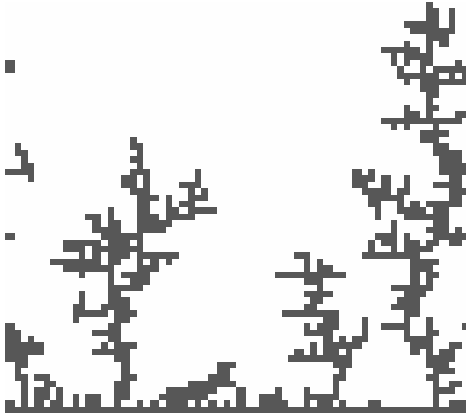


Figure 4: 2d model example in a system of size 64×64

- populate layer zero of the mesh with a surface (3d) or line (2d) of filled sites.
- release a walker at some fixed height
- generate a random direction to move the particle using equations 2
- if particle is adjacent to a filled site, it sticks, then release a new walker
- otherwise continue to move existing walker
- if height of maximum stuck particle exceeds box height, then stop.

The model is easily implemented in any programming system, but for efficiency we use an optimised C++ program that can support relatively large simulated box sizes in arbitrary dimensions.

3 Results

Earlier work [17, 18] studied a related diffusion model in a 2-dimensional system. Figure 4 shows the simple trees that grow from the “line” at the base of a 2-dimensional system. Tree structures form and grow from the initially filled-in line of sites along the base. We might reasonably expect similar tree-like structures in a 3-dimensional model system.

In 3-dimensions the model produces more complex and interlocking trees than can form in a 2-dimensional system. Figure 5 shows typical final configurations – when the highest growing structure has reached the top of the system box. The systems shown are for different values of the Peclet number. As can be seen, at very low Peclet numbers the particles fall slowly and diffuse predominantly in horizontal directions. This gives rise to a relatively small number of tall, narrow trees with single roots. At high Peclet numbers the particles fall and diffuse relatively little in the horizontal direction. This gives rise to denser squatter trees, and we speculate that percolation effects lead to individual trees touching and growing into a single structure at intermediate heights. This gives rise to structures that have multiple root points on the base surface.

The model is computationally expensive, since it requires a lot of generated random numbers and to obtain good statistical accuracy on measured properties large system sizes and many independently started runs were necessary. It was not obvious *a priori* if the model was self averaging in the sense that it was preferable to run fewer large system sizes or many smaller sizes. Figure 6 shows the system density measured as a function of height for various combinations of base (width w times breadth b) and height (h or z) sizes at a Peclet number of $P_e = 1$. Density $\rho(z)$ is defined as:

$$\rho(z) = \frac{1}{w \times b} \sum_{x,y} S_{x,y} \quad (3)$$

where the site cells $S_{x,y,z}$ take the values of 0 (unfilled) and 1 (filled). The density was found to vary considerably with Peclet number as discussed below. However firstly, Figure 6 shows the form of the density profile curves with height. Near the base surface the density is at a maximum, and it tails off with rising height until it reaches a sharp cutoff, that is influenced by the height of the simulated box size. There is effectively a penetration depth effect shown by the density cutoff near the top of the box. Generally taking a box height twice the base length gave good statistical properties for the simulations of the model reported in this present paper, although there is scope to explore limiting effects on the penetration depth by simulating very much deeper boxes.

In Figure 6 cases B,C used the same height but different base sizes and produced nearly identical density profiles. Cases E,F do show the model is more sensitive if the box height is bigger. Case A shows that a base size of 32×32 is too small to adequately sample the model statistical properties. A very large box base size of 1024×1024 did not give appreciably different statistical properties than did smaller base sizes, and therefore most of the work reported in this paper was performed with 100 independent runs or more, on box sizes of base 128×128 and height 256 (Case E).

Using this reference size, one can ascribe different height

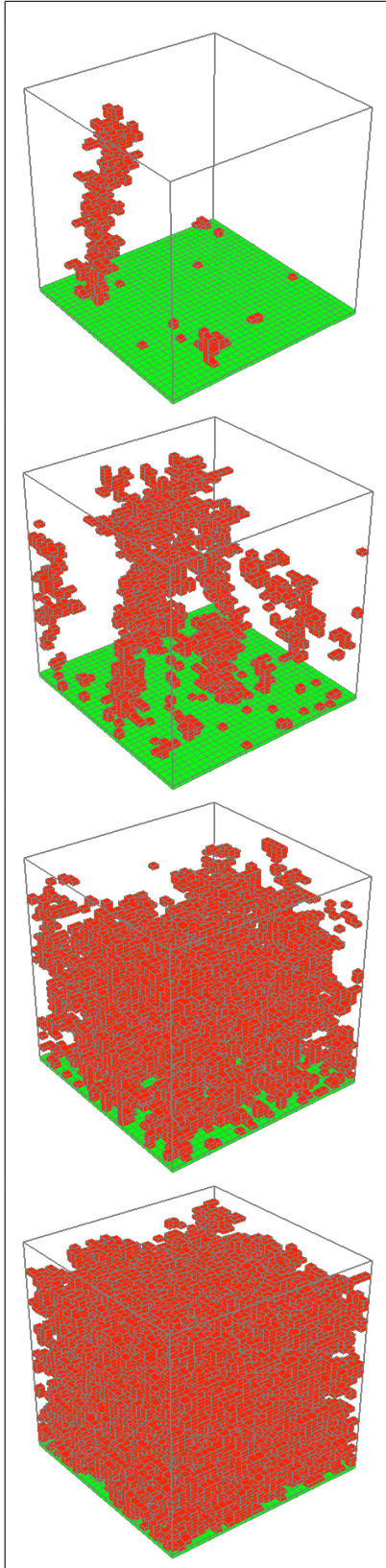


Figure 5: Configuration when final walker added (before filling a $32 \times 32 \times 64$ cell box) at Peclet numbers of: 0.01; 0.10; 1.00; 10.0

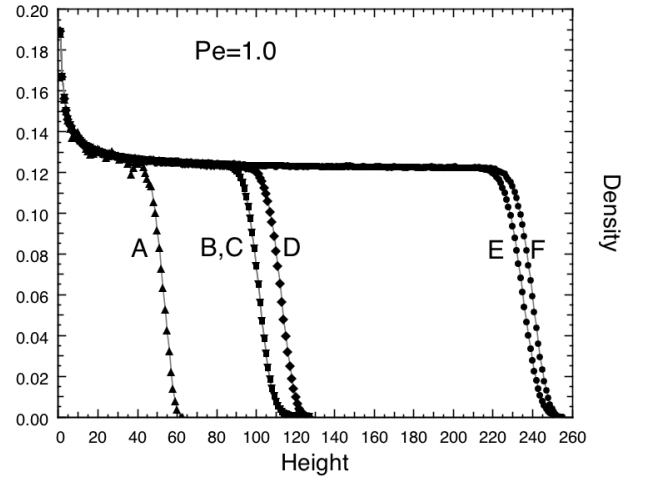


Figure 6: Density profile as a function of height, with $P_e = 1$, for A) $32 \times 32 \times 64$; B) $512 \times 512 \times 128$; C) $1024 \times 1024 \times 128$; D) $64 \times 64 \times 128$; E) $128 \times 128 \times 256$; F) $64 \times 64 \times 256$.

regions to the model. At height of zero, the model is strongly influenced by the completely filled in surface layer. At heights $\approx 2 - 150$ the density tails off fairly smoothly to a limiting value. Above this height, the structures are “incomplete” in the sense that had the box size been higher and the simulation run for longer then more walkers would have penetrated to lower depths and changed the statistics.

Using these empirical observations to scope more extensive runs, Figure 7 shows the density curves for various Peclet numbers. High Peclet number leads to more rapidly falling particles and more dense structures. This manifests itself as the systematic variation in the limiting density values – before finite box heights dominate near the top of the simulation box.

It is difficult to devise an automatic algorithm to compute the penetration depth range – the s-shaped part of the density curves. A manual inspection suggests the useful cutoff height increases with Peclet number however. The limiting density values were measured from the height range 100 – 150 and weighted least-squared fits. This data is shown in Figure 8. The limiting density ρ_{lim} is shown plotted against the Peclet number, and the inset plot is on a log-log scale. This suggests that a power-law scaling relationship of the form $\rho \approx P_e^\nu$ is obeyed - but only in the limit of low Peclet number. Above a critical value of the Peclet number of approximately $P_e^* \approx 0.75$, this power-law breaks down and the behaviour is not a simple function easily identified.

The conventional analysis of the density curves focuses on the low height regime. At low heights, the structures are arguably complete. Even with larger box heights and longer simulation runs, fresh particle walkers are very un-

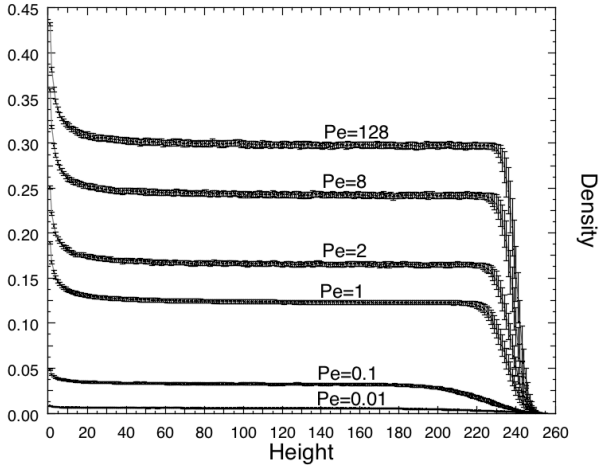


Figure 7: Density profile as a function of height, for $128 \times 128 \times 256$ systems at various Peclet numbers, each curve averaged over 100 independent runs with uncertainties as shown..

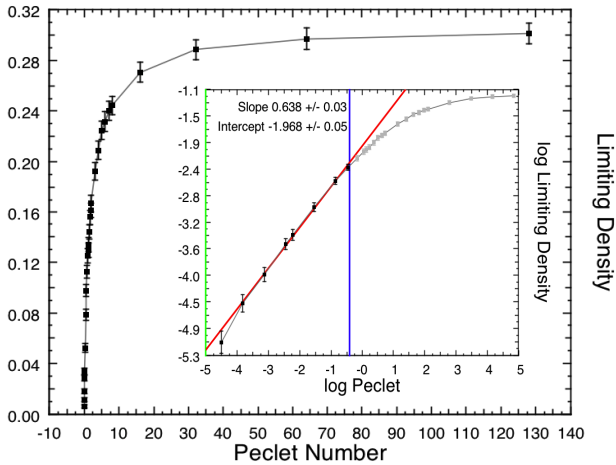


Figure 8: Scaling - log-log fit to the low-Peclet regime of the limiting-density $\rho(h \rightarrow 0)$ vs P_e for heights of 100-150 in a $128 \times 128 \times 256$ box.

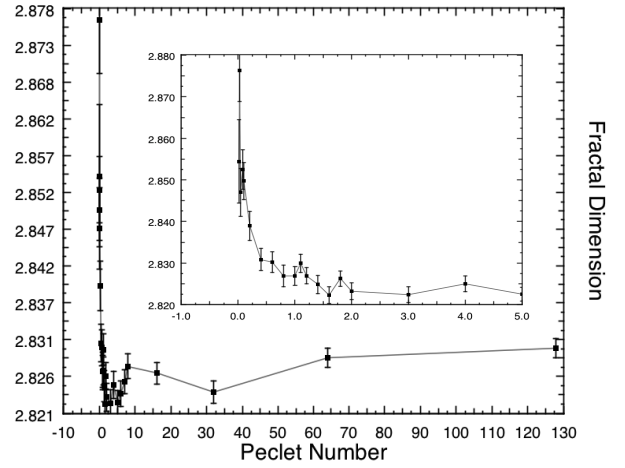


Figure 9: Computed Fractal Dimension as a function of Peclet number.

likely to penetrate to these heights. Consequently we can use the low height regime of the density to computed tentative fractal dimensions of the structures. Fitting a power law of the form:

$$\rho \approx z^{-\alpha} \quad (4)$$

where the fractal or Hausdorff dimension is defined as $d_f = d - \alpha$, where d is the Euclidean embedding dimension of $d \equiv 3$ for the work reported here.

Figure 9 shows the variation of the fractal dimension with Peclet number and the inset shows a blown-up region at low values of P_e . This suggests different Peclet number regimes, and again a transition at $P_e \approx 0.75 - 1$ where d_f drops monotonically, followed by a trough and subsequent convergence to a stable limiting value.

The model shows some complex behaviour as the Peclet number is varied and we speculate that these are due to the changing morphology of the tree-like structures that grow from the surface base.

4 Cluster Morphology

One approach to analysing the structure morphology is to examine the separate clusters or trees that have grown. Figure 10 shows the biggest, second-biggest clusters as well as the monomers and all the trees labelled by colour for a final configuration system snapshot, at a Peclet number of 1.

The tree-like structures can be quite large and have different morphologies depending upon the Peclet number. Figure 1 shows labelled clusters for a Peclet value of 0.1 – they are taller, less squat and sparser than those shown for higher Peclet number. We can automatically identify the component particles in the system according to how

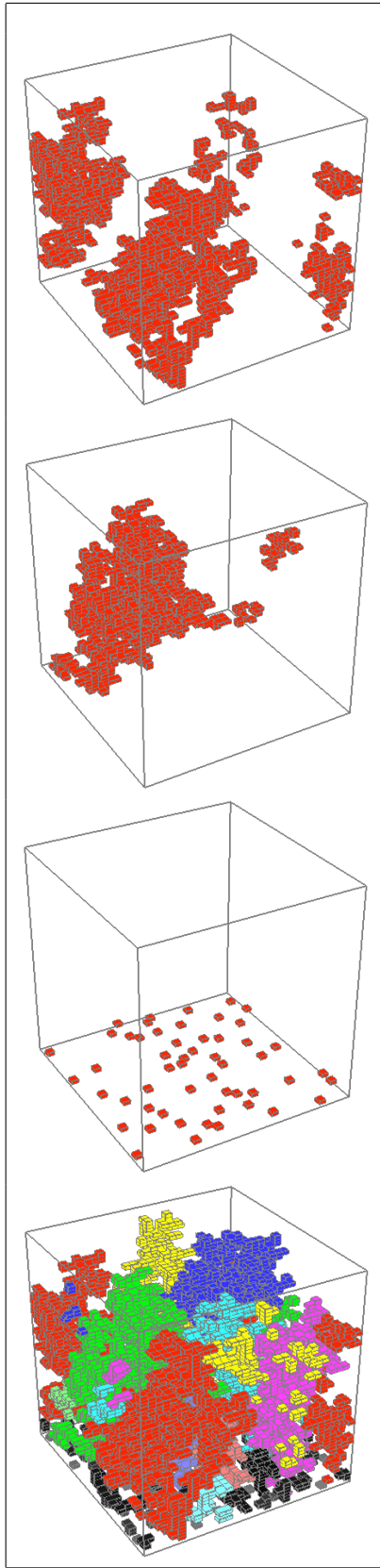


Figure 10: The largest cluster; second-largest cluster; monomers; and labelled set of all cluster trees for Peclet number of 1.

they are connected and thus automatically count the cluster/ tree statistics.

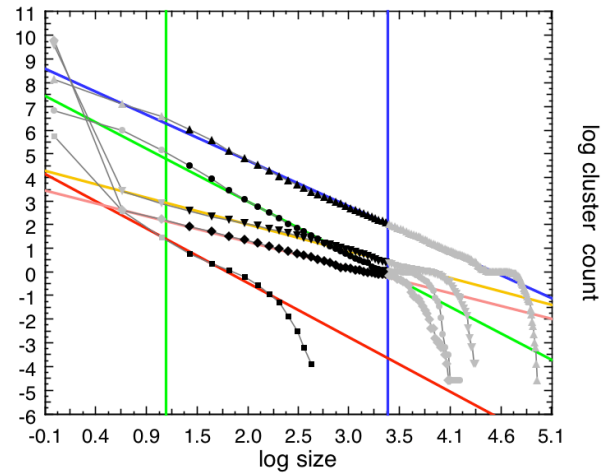


Figure 11: Cluster Numbers vs Cluster Size on log-log scale with slope m in linear region. Curves represent Peclet numbers of 0.01, 100, 10, 0.1, 1.0 from top to bottom, in the mid region shown.

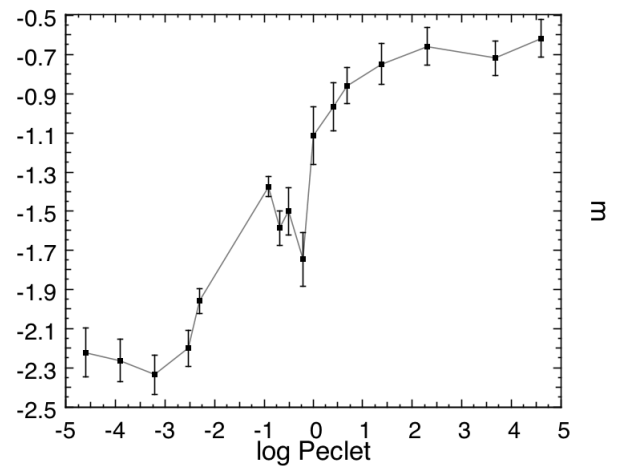


Figure 12: Cluster Numbers vs Cluster Size on log-log scale with slope m in linear region.

Figure 11 shows the cluster count histogram for different cluster sizes built up using many independent runs and shown for five different Peclet numbers. There is a linear region in the log-log plots again suggesting a power law behaviour. Note that there is a cross-over in the curves with cluster count first rising with Peclet number up to a value of around $P_e = 1$, then subsequently falling at high Peclet numbers. Fitting a power m to the linear region of these curves gives rise to Figure 12. This plot shows what appears to be a phase transition at a Peclet number again of around $0.75 - 1$ and a divergence in what is otherwise apparently an s-shaped curve.

These plots – and the error bars shown – are based on 100

independent runs. The sensitivities to the choice of linear region in Figure 11 are what has given rise to the larger error bars in Figure 12.

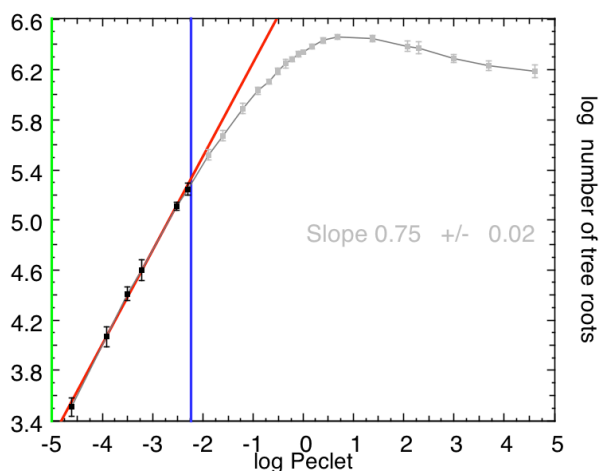


Figure 13: Count of the number of tree roots, adhering to the surface vs the Peclet number – on a log-log scale, with fitted slope in the linear regime.

We speculate that the morphology of the tree structures is strongly affected by percolation and by growing trees touching one another as they rise from the base, and subsequently being “one tree” single structures. This can be investigated quantitatively by measuring the number of tree roots as it changes with the Peclet number. Figure 13 shows a log-log scale plot of the number of tree roots (as measured from a 2-d slice immediately above the base surface) and the Peclet number. There appears to be a power-law regime at low Peclet number, followed by a peak, followed by a converging regime. The linear limit of the log-log plot of Figure 13 at low Peclet number shows convincing evidence again of power-law behavior (with exponent 0.75 ± 0.02).

5 Summary and Conclusions

We have developed a model of directed diffusion to deposit particles on a flat surface. The model is controlled by a single parameter – the Peclet number – and exhibits considerable richness of tree-like structures formed. At high Peclet number it appears percolation effects dominate [33] and the trees merge to form a single sponge-like structure with measurable fractal dimension.

We have shown that the Peclet number is a useful parameter and that several properties of the model can be related to power-laws in this parameter – at least as limiting behaviour. We have identified what appears to be a phase transition in the model at a Peclet number of between $P_e \approx 0.75 - 1$. We speculate that various morpho-

logical changes that manifest themselves in changes in the number and structure of tree-clusters formed are caused by percolation effects as the structures grow from the surface base of the model.

This model, although simplified, may have applications – at low Peclet number - for electro-deposition application problems or more generally for studying effects in coatings, spongi-form structures and other epitaxial growth problems. Other application areas for future study could use directed-diffusion with jets and nozzles rather than the steady particle flux model we have employed. Another variation would involve multiple particle types [34] to study tracer diffusion and competitive deposition effects.

References

- [1] Schulte, A., Chow, R.H.: A simple method for insulating carbon-fiber microelectrodes using anodic electrophoretic deposition of paint. *Anal. Chem.* **68** (1996) 3054–3058
- [2] Li, Y., Vu, N., Kim, A.S.: 3-d monte carlo simulation of particle deposition on a permeable surface. *Desalination* **249** (2009) 416–422
- [3] Ugur, S.S., Sarnsik, M., Aktas, A.H., Ucar, M.C., Erden, E.: Modifying of cotton fabric surface with nano-zno multilayer films by layer-by-layer deposition method. *Nanoscale Res. Lett.* **5** (2010) 1204–1210
- [4] Tokar, V., Dreyse, H.: A lattice gas model of strained epitaxy and self-organization of small clusters. *Computational Materials Science* **24** (2002) 72–77
- [5] Jettestuen, E., Jamtveit, B., Podladchikov, Y., deVilliers, S., Amundsen, H., Meakin, P.: Growth and characterization of complex mineral surfaces. *Earth and Planetary Science Letters* **249** (2006) 108–118
- [6] Kawabuchi, Y., Sotowa, C., Kishino, M., Kawano, S., Whitehurst, D.D., Mochida, I.: Chemical vapor deposition of heterocyclic compounds over active carbon fiber to control its porosity and surface function. *Langmuir* **13** (1997) 2314–2317
- [7] Matsushita, M., Sano, M., Hayakawa, Y., Honjo, H., Sawada, Y.: Fractal structures of zinc metal leaves grown by electrodeposition. *Phys. Rev. Lett.* **53** (1984) 286–289
- [8] Ackland, G., Tweedie, E.: Microscopic model of diffusion limited aggregation and electrodeposition in the presence of leveling molecules. *Phys. Rev. E* **73** (2006) 011606–1–5

- [9] Das, A., Mallik, A., Ray, B.: Chronoamperometric and structural studies of potentiostatically deposited nickel in presence of ultrasound. In: Proc. International Conference on Recent Trends in Materials and Characterization (RETMAC -2010), NIT, Suratkal, Karatna (2010) 1–6
- [10] T.A.Witten, L.M.Sander: Diffusion Limited Aggregation, a Kinetic critical Phenomenon. *Phys.Rev.Lett.* **47** (1981) 1400–1403
- [11] Meakin, P.: Diffusion controlled cluster formation in 2-6 dimensional space. *Phys. Rev. A* **27** (1983) 1495–1507
- [12] Schwarzer, S., Lee, J., Bunde, A., Havlin, S., Roman, H.E., Stanley, H.E.: Minimum growth probability of diffusion-limited aggregates. *Phys. Rev. Lett.* **65** (1990) 603–606
- [13] Sze, S., Ng, K.K.: *Physics of Semiconductor Devices*. 3rd edition edn. Number ISBN 9780471143239. Wiley (2007)
- [14] Meakin, P.: Diffusion-controlled deposition on fibers and surfaces. *Phys. Rev. A* **27** (1983) 2616–2623
- [15] Meakin, P.: Diffusion-controlled deposition on surfaces: Cluster-size distribution, interface exponents, and other properties. *Phys. Rev. B* **30** (1984) 4207–4214
- [16] Park, W., Yi, G.C., Jang, H.: Metalorganic vapor-phase epitaxial growth and photoluminescent properties of ZnO thin films. *Applied Physics Letters* **79** (2001) 2022–2024
- [17] Douglas, I.S.: Vapour phase epitaxy: A diffusion limited aggregation phenomenon. Technical report, Edinburgh Parallel Computing Centre (1990)
- [18] Critchley, O.J.F.: Vapour phase epitaxial growth. Technical report, Edinburgh Parallel Computing Centre (1991)
- [19] Peltomaki, M., Hellen, E.K.O., Alava, M.J.: No self similar aggregates with sedimentation. *Journal of Statistical Mechanics: Theory and Experiment* (2004) P09002
- [20] Hawick, K.: Simulating and visualising sedimentary cluster-cluster aggregation. In: Proc. International Conference on Modeling, Simulation and Visualization Methods (MSV'10). Number CSTN-012, Las Vegas, USA (2010) MSV3277.
- [21] Russel, W., Saville, D., Schowalter, W.: *Colloidal Dispersions*. Cambridge University Press (1989) ISBN 0-521-34188-4.
- [22] Barenblatt, G.I.: *Scaling*. Cambridge University Press (2003) ISBN 0-521-53394-5.
- [23] P.Meakin, M.H.Ernst: Scaling in Aggregation with breakup simulations and mean field theory. *Phys.Rev.Lett.* **60** (1988) 2503–2506
- [24] Family, F., Meakin, P.: Scaling of the droplet size distribution in vapor-deposited thin films. *Phys. Rev. Lett.* **61** (1988) 428–431
- [25] Meakin, P.: *Fractals, Scaling and Growth far From Equilibrium*. Number ISBN 0-521-45253-8. Cambridge University Press (1998)
- [26] Vicsek, T.: *Fractal Growth Phenomena*. World Scientific (1989)
- [27] Asnaghi, D., Carpineti, M., Giglio, M., Sozzi, M.: Coagulation dynamics and aggregate morphology in the intermediate regimes between diffusion-limited and reaction-limited cluster aggregation. *Phys. Rev. A* **45** (1992) 1018–1023
- [28] Maloy, K.J., Feder, J., Jossang, T.: Viscous fingering fractals in porous media. *Phys. Rev. Lett.* **55** (1985) 2688–2691
- [29] Park, W., Kim, D., Jung, S.W., Yi, G.C.: Metalorganic vapor-phase epitaxial growth of vertically well-aligned ZnO nanorods. *Applied Physics Letters* **80** (2002) 4232–4234
- [30] Mishra, K., Paramguru, R.: Surface modification with copper by electroless deposition technique: An overview. *African Journal of Pure and Applied Chemistry* **4** (2010) 87–99
- [31] Vasco, E., Zaldo, C.: Growth Kinetics of Epitaxial Y-Stabilized ZrO₂ films deposited on InP. *J.Phys.: Condens. Matter* **16** (2004) 8201–8211
- [32] Gonzalez, A.E.: Colloidal Aggregation in the presence of Gravity. In: *Nanotech 2001 - Technical Proc. of the 2001 Int. Conf. on Computational Nanoscience and Nanotechnology*, Computational Publications (2001) 49–52
- [33] Cheng, J., Zhao, M., Yuan, X., Zhao, L., Huang, D., Zhou, S.: The percolation properties of fractal aggregation. *Physica A* **343** (2004) 335–342
- [34] Rodriguez-Romo, S., Tchijov, V., Ibanez-Orozco, O., Castano, V.M.: Growth probability in bicolored diffusion limited aggregation. *Physica A* **In Proof** (2004)